OPTO-ELECTRONICS REVIEW **12**(4), 411–416

An attempt to design room-temperature-operated nitride diode VCSELs

P. MAĆKOWIAK[1], R.P. SARZAŁA[1], M. WASIAK[1], and W. NAKWASKI[*1,2]

[1]Laboratory of Computer Physics, Institute of Physics, Technical University of Łódź
219 Wólczańska Str., 93-005 Łódź, Poland
[2]Center for High Technology Materials, University of New Mexico,
1313 Goddard SE, Albuquerque, NM, USA

The new modified structure of nitride diode vertical-cavity surface-emitting lasers (VCSELs) of anticipated high-performance low-threshold room-temperature operation is presented. Two essential structure modifications are proposed in this new design. First, tunnel junctions and a semi-transparent contact are used to enhance uniformity of the current injection into a VCSEL active region. Second, a new built-in radial waveguiding mechanism is introduced within the output distributed Bragg reflector. According to simulation results, the radius of the active region may be dramatically reduced in this new VCSEL design, even to just 1 μm, without a significant increase in the cavity optical losses. Hence, using this new proposed design, manufacturing low-threshold, electrically-driven, room-temperature-operated nitride VCSELs may become possible even at the current, still immature, development stage of nitride technology.

Keywords: nitride diode lasers, nitride vertical-cavity surface-emitting lasers, modelling of a room-temperature operation.

1. Introduction

History of nitride diode lasers began in December 1996, when their first continuous-wave (CW) room-temperature (RT) operation was reported [1]. It was obviously an edge-emitting (EE) diode laser. Currently EE nitride diode lasers are already commercially available. However, their another possible configuration, namely the nitride vertical-cavity surface-emitting laser (VCSEL), seems to be much more promising taking into consideration its numerous potential applications. Nevertheless, RT operation of nitride diode VCSELs has not been reported until now at all.

There are many reasons of problems with RT operation of possible nitride diode VCSELs. It is obvious that nitride VCSELs need stronger excitation (exhibit definitely higher lasing thresholds) than nitride EE lasers, disregarding their structures. But one their peculiarity, being a result of special features of nitride materials, plays a special role in an operation of nitride VCSELs. It is definitely a very high electrical resistivity of the p-type nitride materials. Consequently, in typical nitride VCSELs structures with both n-side and p-side annular contacts, current injection into a laser active region is extremely nonuniform: nearly insignificant current density reaches the active-region centre whereas its dramatic increase may be observed with approaching its perimeter. Similar nonuniformity has been reported also for some arsenide and phosphide VCSELs of similar structures. But this effect is much more severe in possible nitride VCSELs. Besides, low-order transverse modes are also not favoured in the standard nitride VCSEL structure because of a lack of any radial waveguiding mechanism (as, e.g., oxide apertures in arsenide VCSELs) discriminating higher-order modes. Accordingly, beneficial single-mode operation on the LP_{01} fundamental mode needs relatively high excitation in possible standard nitride VCSELs and higher-order transverse modes may even exhibit lower lasing thresholds which leads to a possible very disadvantageous multimode operation.

The above situation may be drastically improved by an enhancement of uniformity of current injection into VCSEL active regions and an introduction of an efficient radial built-in waveguiding mechanism which may together considerably reduce the lasing threshold for the fundamental LP_{01} mode. The first improvement may be accomplished by tunnel junctions and/or semi-transparent contacts. There are still, however, some difficulties in creating radial built-in waveguide in nitride VCSELs. It has been easily introduced in arsenide diode VCSELs with the aid of a selective oxidation of the AlAs-rich (AlGa)As layers [2,3]. The oxidation apertures work not only as radial waveguides but they also may funnel current spreading into the central active region. Unfortunately, similar technological structure modification of a laser resonator is not known in possible nitride VCSELs. Therefore in this paper a new

*e-mail: nakwaski@p.lodz.pl

method of an enhancement of uniformity of current injection into the active region (Sect. 2) and new built-in radial optical confinement mechanism (Sect. 3) is proposed. The first is associated with a proper arrangement of tunnel junctions and a semi-transparent contact, the second consists in a modification of the cylindrical part of the output distributed Bragg reflector (DBR). Performance of the above VCSEL structure modifications will be analysed using the comprehensive VCSEL model.

2. Uniformity of current injection

Possible resonator mirrors of nitride VCSELs, even semiconductor ones, are practically electrical isolators. Therefore a double lateral injection scheme (Fig. 1) with the aid of two (p-side and n-side) ring contacts seems to be unavoidable in these devices. As a result, current injection into the centrally located VCSEL active region is extremely nonuniform: hardly any current can reach its broad central part and the current flow through a p-n junction is practically confined to a narrow ring area close to the active-region perimeter. Such a profile enhances unwanted multi-mode operation on higher-order transverse modes. Although this effect is already known in some arsenide and phosphide VCSELs, it is much stronger in nitride ones because of special features of nitrides – extremely high electrical resistivities of p-type nitrides and very rapid temperature changes of nitride refractive indices.

Let us consider the simplest possible structure of nitride VCSELs with two annular contacts. There are two possible methods to enhance uniformity of current injection into VCSEL active regions: with the aid of a semi-transparent upper contacts and/or tunnel junctions. Our detailed comparative analysis (using the methods of computer physics [4]) of many possible VCSEL designs ($\lambda = 400$ nm) reveals that the best results are obtained in the modified nitride VCSEL (Fig. 2). The proposed VCSEL is equipped with a double $In_{0.15}Ga_{0.85}N/In_{0.02}Ga_{0.98}N$ multiple-quantum-well active region, two tunnel junctions (15-nm InGaN heavily doped with Mg and 30-nm GaN heavily doped with Si [5])

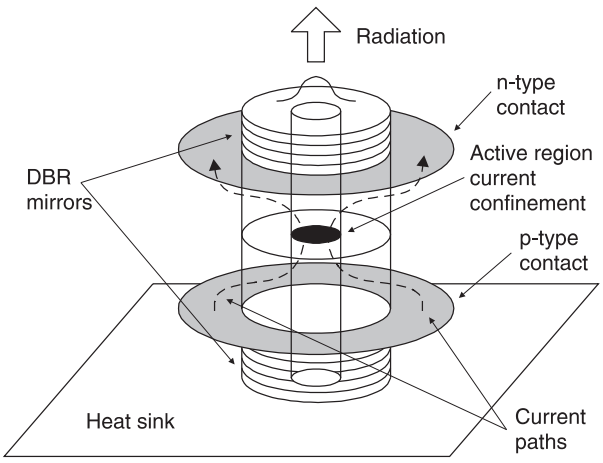

Fig. 1. Double-lateral injection scheme of nitride VCSELs.

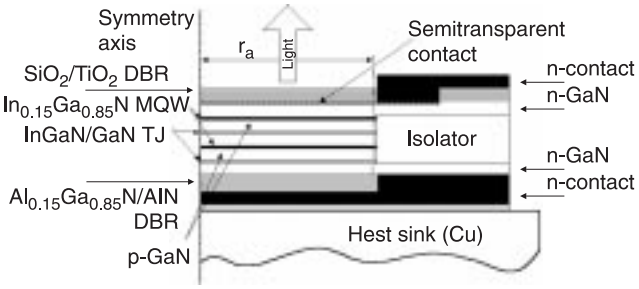

Fig. 2. New proposed design of nitride VCSELs with a double multiple-quantum-well (MQW) active regions, two tunnel junctions (TJs) and a semi-transparent contact.

and a semi-transparent contact (25-nm thick indium tin oxide (ITO) layer [6]). The above laser construction should be carefully designed to place active regions in maxima positions of the optical-intensity standing wave whereas both tunnel junctions and a semi-transparent contact – in its minima ones (Fig. 3).

Let us consider two possible structures of nitride VCSELs: the traditional double-ring contacted (DRC) one without any modifications and the new one with tunnel junctions and a semi-transparent contact (Fig. 2). For their continuous-wave (CW) RT operation, radial p-n junction current density profiles are plotted in Fig. 4 for active-region diameters of 10 μm. As one can see, extremely strong current crowding effect close to the active-region edge occurs in the traditional DRC laser, whereas, in the proposed VCSEL design, nearly perfectly uniform current injection is observed. Uniformity of current injection is improved in the new design mostly because the previous top high-resistivity p-type current-spreading upper layer is replaced in the new design by the n-type GaN layer of resistivity lower by more than two orders of magnitude, which strongly reduces the current crowding effect. As a result,

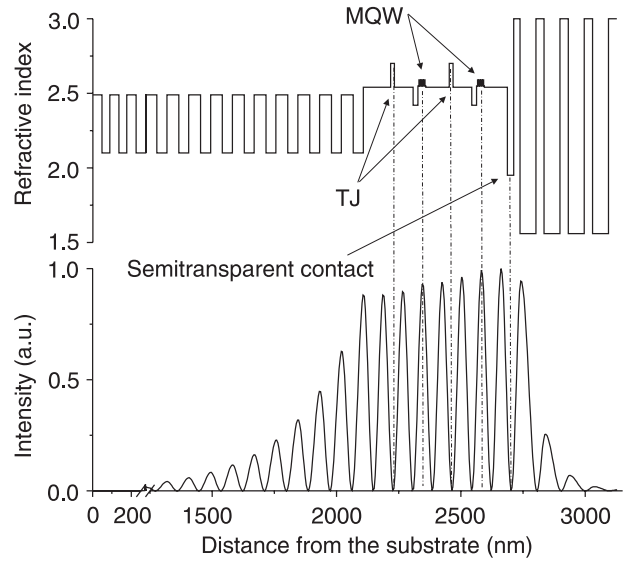

Fig. 3. The intensity standing wave in the propagation direction within the cavity of the VCSEL design shown in Fig. 2. TJ – tunnel junction, MQW – active region.

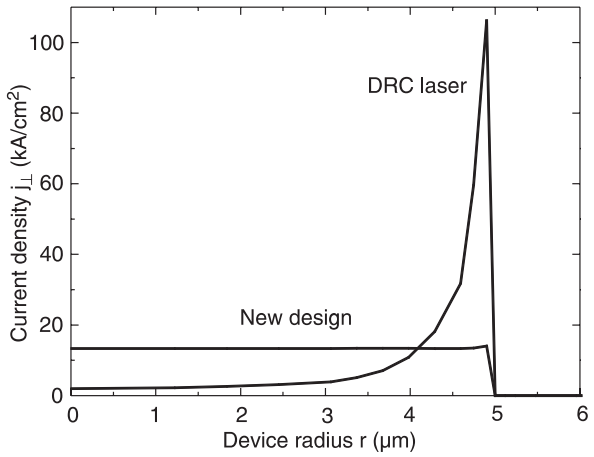

Fig. 4. Radial profile of the p-n junction current density within 10-μm active regions of nitride VCSELs operating CW at RT: the traditional DRC design and the new design.

the high-order LP_{81} transverse mode reaches first the CW RT lasing threshold in the case of the traditional DRC nitride VCSEL whereas the desired fundamental-mode LP_{01} operation is expected in the case of the new modified nitride VCSEL.

3. Built-in radial waveguide

3.1. The theory

Let us consider the performance of various waveguiding effects using the effective frequency method proposed by Wenzel and Wünsche [7]. The optical field $E(r,z,\varphi)$ is assumed to be of the following form

$$E(r,z,\varphi) = f(r,z)\Phi(r)\exp(iL\varphi), \tag{1}$$

where L = 0, 1, 2, ... is the azimuthal mode member.

The above expression enables us to reduce the wave equation within the VCSEL resonator to the following two mutually interrelated, nearly-one-dimensional wave equations along both the axial and the radial directions [7]

$$\left[\frac{d^2}{dz^2} + k_0^2 n_R^2(r,z)\right] f(r,z) = v_{eff}(r) k_0^2 n_R(r,z) n_g(r,z) f(r,z), \tag{2a}$$

$$\left[\frac{d^2}{dr^2} + \frac{1}{r}\frac{d}{dr} - \frac{L^2}{r^2} + v_{eff}(r) k_0^2 \left\langle n_R n_g \right\rangle_r\right] \Phi_L(r) = v k_0^2 \left\langle n_R n_g \right\rangle_r \Phi_L(r), \quad L = 0, 1, 2,\ldots \tag{2b}$$

where v_{eff} stands for the effective frequency, $k_0 = \omega_0/c$ is the vacuum wave number and ω_0 is the real-valued nominal angular frequency corresponding to the desired periodicity of DBR mirrors. n_R and n_g are the complex refractive phase and group indices, respectively, evaluated at the nominal angular frequency ω_0. The dimensionless complex parameter v plays the role of an eigenvalue and is defined as

$$v \equiv 2\frac{\omega_0 - \omega}{\omega_0}. \tag{3}$$

Outgoing plane waves are assumed as boundary conditions for the bottom and the top resonator surfaces, whereas, for sufficiently large radial distances, a cylindrical outgoing waves are assumed. The solving algorithm of the above Eqs. (1) and (2) needs a self-consistent procedure because the effective frequency v_{eff} is present in both of them. The lasing threshold for a given radiation mode is found when corresponding propagation constant becomes real (so its imaginary part vanishes).

Following the previous section, a step gain profile of the diameter $2r_c$ (equal to the active-region diameter) is assumed in the analysis. Only the pulse RT lasing operation is considered to simplify calculations. However, one should remember that nitrides exhibit very strong temperature dependence of their refractive indices [8], so if current paths are properly designed, the temperature distribution during the CW operation could cause an additional strong thermal focusing effect, improving radial waveguiding properties. Thank to the above simplifications, any observed improvement in performance characteristics of the modified laser will definitely follow from an improvement in radial optical confinement itself.

To compare confinement of an optical field in possible VCSEL structures of nitride diode lasers, the effective modal threshold gain G_{LM} is introduced. From the definition, the effective modal gain G_{LM} of a given radiation LP_{LM} mode is an average optical material gain (with optical losses being taken into account additionally) in the laser structure weighted by an intensity distribution of the mode [9]

$$G_{LM} = \frac{\int_0^{r_s}\int_0^{L_L}\int_0^{2\pi} I_{LM}(r,z,\varphi)[g(r,z,\varphi) - \alpha(r,z,\varphi)]r\,dr\,dz\,d\varphi}{\int_0^{r_s}\int_0^{L_L}\int_0^{2\pi} I_{LM}(r,z,\varphi)r\,dr\,dz\,d\varphi}. \tag{4}$$

where r_s stands for the structure radius, L_L is the resonator length, I_{LM} is the intensity distribution of the radiation coupled into the LP_{LM} mode, and g and α are the spatial distributions of optical gains and losses, respectively. So, G_{LM} takes into account in a natural way all areas where there is a gain of the optical intensity and also all areas where radiation is absorbed or lost, but, in both cases, proportionally to the local mode intensity. When the distribution of mode intensity is not correlated with gain areas and/or the mode spreads considerably into absorption areas, the mode needs higher material optical gain in quantum wells to be excited.

Table 1. VCSEL parameters assumed in the calculations: d are the layer thicknesses (in DBR structures for both alternating layers, respectively), n_R are the refractive indices, n_g are the group refractive indices, α are the absorption coefficients, DBR period or QW numbers are given in brackets (Data are taken from: [a]Ref. 12, [b]Ref. 13, [c]Ref. 14, [d]Ref. 15, [e]Ref. 16 where not indicated, references to the data can be found in our previous publications [10,11]).

Layer	d (nm)	n_R	n_g	α (cm^{-1})
SiO_2 TiO_2 (6.5) DBR Ag coating	64.10 33.30 200.00	1.56[a] 3.00[a] 0.173[a]	1.61[a] 5.00[a] 0.441[a]	10 612610
n-GaN spacer	74.16	2.54[b]	3.44[b]	10
n-GaN Al_xO_y	9.15 15.00	2.54[b] 1.55[e]	3.44[b] 1.575[e]	10 10
n-GaN spacer	58.24	2.54[b]	3.44[b]	10
n-GaN spacer	141.56	2.54[b]	3.44[b]	10
$In_{0.15}Ga_{0.85}N$ QW (5)	3.50	2.55[c]	2.55[c]	–2000
$In_{0.02}Ga_{0.98}N$ barrier (4)	3.50	2.59[d]	3.83[d]	10
p-$Al_{0.2}G_{0.8}N$ blocking layer	20.00	2.42[b]	3.45[b]	10
p-GaN	75.16	2.54[b]	3.44[b]	10
p-InGaN:Mg^{++}	15.00	2.70[b]	4.50[b]	150
n-GaN:Si^{++}	30.00	2.54[b]	3.44[b]	150
n-GaN	158.88	2.54[b]	3.44[b]	10
AlN $Al_{0.15}Ga_{0.85}N$ (17.5) DBR	47.60 40.20	2.10[b] 2.49[b]	2.67[b] 3.53[b]	10

3.2. The structures

The new structure of a nitride VCSEL proposed in Sect. 2 is very complicated. Therefore we have decided to test usability of our new radial optical waveguiding mechanism in much simpler VCSEL structures, assuming, however, perfect uniformity of current injection confirmed for this new VCSEL design. Four possible simple structures of nitride VCSELs are schematically shown in Fig. 5. In all VCSEL designs, six and a half pairs of the dielectric SiO_2/TiO_2 DBR are used as upper resonator mirrors, whereas seventeen and a half pairs of the semiconductor $AlN/Al_{0.15}Ga_{0.85}N$ DBR are applied on the bottom of their structures as output resonator mirrors. The desired emission wavelength in all designs is assumed to be 400 nm. All the layers between the bottom and the top DBR resonator mirrors comprised a 3λ cavity. As the active region, five 3.5 nm $In_{0.15}Ga_{0.85}N$ quantum wells (QWs) separated by 3.5-nm $In_{0.02}Ga_{0.98}N$ barriers are chosen. The detailed assumptions regarding the active region and the cavity as well as the reasons for choosing the above materials in DBRs are explained in our earlier publications [10,11]. Table 1 lists all the parameters used in our calculations (where not indicated, the references can be found in Refs. 10 or 11).

In all four VCSEL structures under consideration, a classical double lateral injection scheme is applied. The first standard structure, labelled 'STD', has no additional built-in radial optical confinement. The second one (labelled 'etched DBR'') has a pillar shaped upper dielectric DBR, which could be fabricated by selective dry etching.

The third structure is based on the second one. Its manufacturing is as follows. First, the upper DBR should be etched to form a pillar leaving only the last low-index bottom SiO_2 layer intact. Then, on the top of the exposed part of that layer, the second low-index SiO_2 layer of the same thickness as the TiO_2 layer near the pillar should be deposited again (Fig. 5), so the external SiO_2 layer is as thick as both together the internal SiO_2 and TiO_2 layers. The refractive index step between SiO_2 and TiO_2 seems to be high enough to ensure efficient radial waveguiding, but the effect of optical confining can be enhanced if the exposed part of the thickened SiO_2 layer is additionally covered by a highly reflecting layer. In our simulation, we chose a silver metallic coating for this but similar results have been obtained also for an aluminium layer and a dielectric DBR stack. The key feature of the coating layer mentioned above is its reflectivity, which should be at least around 90%.

The last structure, labelled 'oxidized aperture', is a hypothetical structure with both optical and electrical radial confining mechanisms taken, only for comparison, from arsenide VCSEL structures. The 'oxidized aperture' is placed in the anti-node position of a standing wave within the resonator to create more efficient optical confinement.

3.3. The results

Figure 6 presents the RT material gain within VCSEL QWs necessary for the fundamental LP_{01} mode to reach its lasing threshold plotted as a function of the radius r_c of the active region, for all structures considered. It has been found that

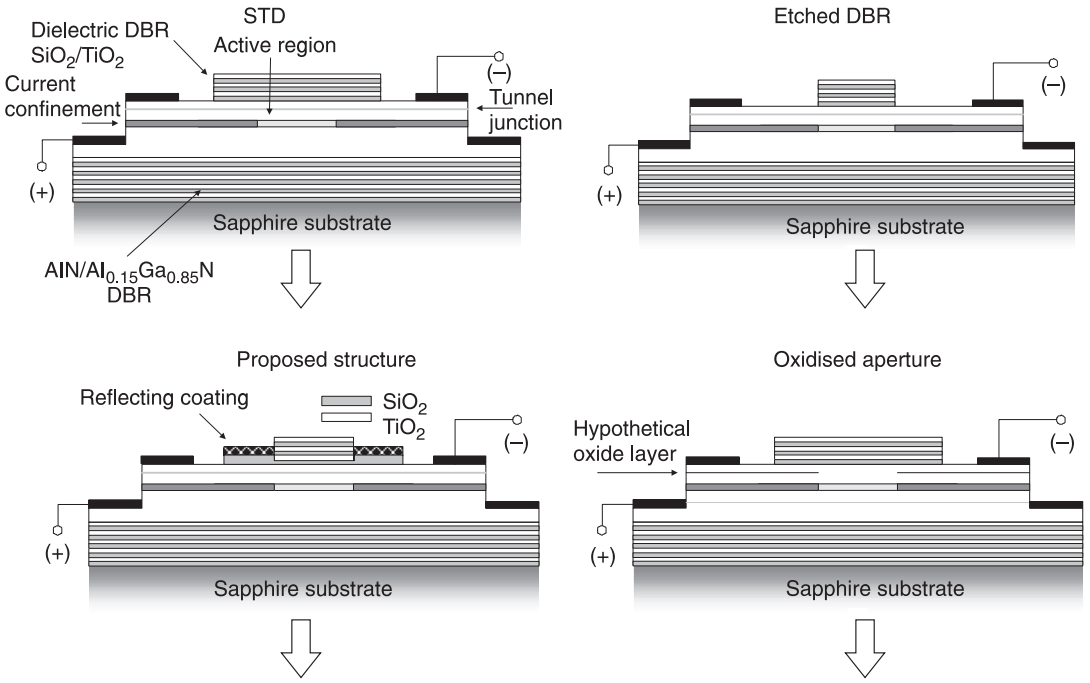

Fig. 5. Schematic diagram of the analysed structures of output DBR mirrors in nitride VCSELs.

the fundamental LP_{01} mode exhibits the lowest lasing threshold in all of them. As one can see, it is almost stable and practically the same for radii larger than about 5 μm, while for smaller radii, it starts increasing dramatically. This could be explained in the case of the standard STD VCSEL structure by a change in the radial mode profile (see inset in Fig. 6). The smaller the radius of the active region, the more the mode spreads into the high absorption lateral areas and, in this way, diffraction optical losses and, subsequently, lasing thresholds are increased, so higher material optical gain within VCSEL QWs is necessary for the LP_{01} mode to overcome these additional optical losses and to reach its lasing threshold.

In all remaining structures, equipped with some built-in radial optical confinement mechanisms, an increase in the threshold gain in QWs observed for the smaller r_c is a result of increasing edge losses, proportional to $\ln[(R_F R_R)^{-1}]$, where R_F and R_R are the reflectivity coefficients for the front and the rear DBR mirrors, respectively. For $r > r_c$, R_F is equal to as much as 99.5% for the 'oxidized aperture' structure, to about 90% for our new proposed structure and to only about 50% for the 'etched DBR' structure. That is why increasing edge losses are followed by increasing lasing thresholds for smaller active regions. However, if the waveguide is properly designed, this phenomenon may occur for much smaller radii, which may enable a reduction of the threshold current.

It is difficult to introduce radial waveguiding mechanism into cavities of nitride VCSELs. Therefore we have given our attention to the upper DBR. If it is etched to form a pillar above the active region (Fig. 6, 'etched DBR'), one may expect a strong radial waveguiding effect to occur, as the refractive-index step between TiO_2 and air is very high (around 2). Our simulations, however, revealed that only a small and discouraging improvement is observed in this case (c.f. Fig. 6, curve 'etched DBR'). This may be explained by considering optical losses in the cavity. The

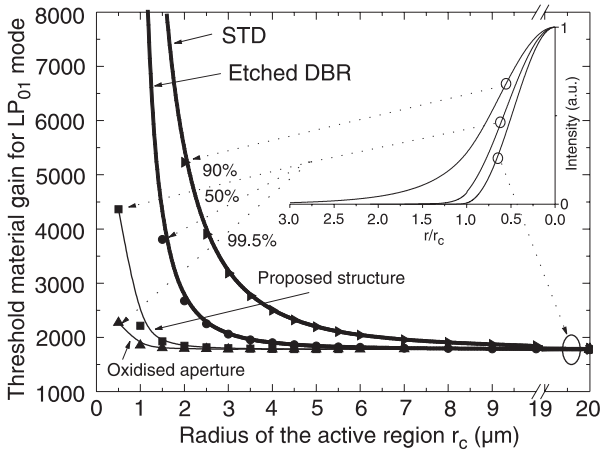

Fig. 6. RT threshold material gain within QWs of the VCSEL structures under consideration (see Fig. 5) versus the radius r_c of the active region (equal to the radius of the built-in radial optical confinement in all structures but the STD one). The inset shows radial intensity LP_{01} mode profiles for all structures plotted for radii of the active region less than 2 μm and equal to 20 μm. For small active regions, an optical field penetrates passive areas considerably in the case of the traditional 'STD structure', whereas this penetration is much shallower for structures with a built-in radial optical confinement, i.e., the 'etched DBR' structure, the new proposed structure and the hypothetical 'oxidized aperture' structure (the corresponding curves are very similar). In the latter case, reflectivity coefficients (in per cent) in the area $r > r_c$ are indicated. For large active regions, optical-field profiles are practically identical in all four considered structures.

LP_{01} mode penetrates the lateral ($r > r_c$) regions. This penetration becomes considerable when the radius of the active region is reduced below 5 μm [11]. When both lateral intensity tails are considerably reduced after reflection (as in the 'etched DBR' structure), the effective reflection coefficient for the whole mode is also reduced, so its optical losses are increased. Therefore, to improve radial optical confinement for a specific mode, it is crucial to increase the reflection coefficient for the tail parts of the mode intensity to a similar value as that of the central ($r < r_c$) part of the resonator. It can be realized, e.g., by forming a highly reflecting metallic layer above the optical confinement layer in close proximity to the etched pillar of the dielectric DBR; and, in fact, it is clearly seen in Fig. 6, that the reflecting metallic layer in the 'proposed structure' distinctly improves the optical confinement.

The best optical confinement could, however, be achieved if the confining layer is placed within the cavity (c.f. Fig. 6, curve 'oxidized aperture'). In the case of arsenide VCSELs, this is easily realized using the selective radial oxidation of AlAs layers. Unfortunately, in the case of nitrides, a similarly simple process is not known at the current stage of technology, although application of photonic crystals may enable a radical improvement in future. Here, in Fig. 6, we show the results of the calculations carried out for the hypothetical structure of nitride VCSELs with an oxidized aperture only for comparison of efficiencies of the optical confinements.

4. Conclusions

The new modified structure of nitride vertical-cavity surface-emitting lasers (VCSELs) is presented. Two essential structure optimisations are proposed in this new design. First, tunnel junctions and a semi-transparent contact are used to enhance uniformity of the current injection into a VCSEL active region. Second, a new built-in radial waveguiding mechanism is introduced within the output distributed Bragg reflector. According to simulation results, the radius of the active region may be dramatically reduced, even to just 1 μm, without a significant increase in the cavity optical losses. Hence, using this new design with both the above structure modifications, manufacturing low-threshold, electrically-driven, room-temperature-operated nitride VCSELs may become possible even at the current, still immature, development stage of nitride technology.

Radial waveguiding mechanism built-in within a VCSEL resonator has been proved to work more efficiently than the one introduced to resonator mirrors. Therefore photonic band-gap materials may enable manufacturing the best future structures of nitride VCSELs, where radial optical confinement may be created with the aid of a proper linear defect of a photonic-crystal slab.

Acknowledgements

This work was supported by the Polish Committee for Scientific Research (KBN) grants Nos. 7-T11B-073-21 and 4-T11B-014-25.

References

1. S. Nakamura, M. Senoh, S. Nagahama, N. Iwasa, T. Yamada, T. Matsushita, Y. Sugimoto, and H. Kiyoku, "Room-temperature continuous-wave operation of InGaN multi-quantum-well-structure laser diodes with a long lifetime", *Appl. Phys. Lett.* **70**, 868 (1997).
2. M. Osiński, T. Svimonishvili, G.A. Smolyakov, V.A. Smagley, P. Maćkowiak, and W. Nakwaski, "Temperature and thickness dependence of steam oxidation of AlAs in cylindrical mesa structures", *IEEE Photon. Techn. Lett.* **13**, 687 (2001).
3. W. Nakwaski, M. Wasiak, P. Mackowiak, W. Bedyk, M. Osiński, A. Passaseo, V. Tasco, M.T. Todaro, M. De Vittorio, R. Joray, J.X. Chen, R.P. Stanley, and A. Fiore, "Oxidation kinetics of AlAs and (AlGa)As layers in arsenide-based diode lasers: Comparative analysis of available experimental data", *Semicond. Sci. Technol.* **19**, 333 (2004).
4. M. Osiński and W. Nakwaski, "Three-dimensional simulation of vertical-cavity surface-emitting semiconductor lasers", Chapter 5 in *Vertical-Cavity Surface-Emitting Laser Devices*, edited by H. Li and K. Iga, Chapter 5, Berlin, Springer, 2003.
5. S.R. Jeon, Y.-H. Song, H.J. Jang, G.M. Yang, S.W. Hwang, and S.J. Son, "Lateral spreading in GaN-based light-emitting diodes utilizing tunnel contact junction", *Appl. Phys. Lett.* **78**, 3265 (2001).
6. R.-H. Horng, D.-S. Wuu, Y.-C. Lien, and W.-H. Lan, "Low-resistance and high-transparency Ni/indium tin oxide ohmic contacts to p-type GaN", *Appl. Phys. Lett.* **79**, 2925 (2001).
7. H. Wenzel and H.-J. Wünsche, "The effective frequency method in the analysis of vertical-cavity surface-emitting lasers", *IEEE J. Quantum Electron.* **33**, 1156 (1997).
8. G.Y. Zhao, H. Ishikawa, G. Yu, T. Egawa, J. Watanabe, T. Soga, T. Jimbo, and M. Umeno, "Thermo-optical nonlinearity of GaN grown by metalorganic chemical-vapour deposition", *Appl. Phys. Lett.* **73**, 22 (1998).
9. B. Mroziewicz, M. Bugajski, and W. Nakwaski, *Physics of Semiconductor Lasers*, Amsterdam, North-Holland 1991, Chapter 4.1.8.
10. P. Maćkowiak and W. Nakwaski, "Designing guidelines for nitride VCSELs", *J. Phys. D: Appl. Phys.* **33**, 642 (2000).
11. P. Maćkowiak and W. Nakwaski, "Some aspects of designing an efficient nitride VCSEL resonator", *J. Phys. D: Appl. Phys.* **34**, 954 (2001).
12. E.D. Palik, *Handbook of Optical Constants of Solids*, **1** and **2**, Orlando, Academic 1985.
13. D. Brunner, H. Angerer, E. Bustarret, F. Freudenberg, R. Hoepler, R. Dimitrov, O. Ambacher, and M. Stutzmann, "Optical constants of epitaxial AlGaN films and their temperature dependence", *J. Appl. Phys.* **82**, 5090–5096 (1997).
14. M. Mandy. Y. Leung, A.B. Djurisic, and E.H. Li, "Refractive index of InGaN/GaN quantum well", *J. Appl. Phys.* **84**, 6312–6327 (1998).
15. M.J. Bergmann and H.C. Casey Jr., "Optical-field calculations for lossy multiple-layer $Al_xGa_{1-x}N/In_xGa_{1-x}N$ laser diodes, *J. Appl. Phys.* **84**, 1196–1203 (1998).
16. F.A. Kish, S.J. Caracci, N. Holonyak, Jr., J.M. Dallesasse, K.C. Hsieh, and M. J. Flies, S.C. Smith, and F.D. Burnham, "Planar native-oxide index-guided $Al_xGa_{1-x}A$-GaAs quantum well heterostructure lasers", *Appl. Phys. Lett.* **59**, 1755–1757 (1991).

